

Light noble gases and cosmogenic radionuclides in Estherville, Budulan, and other mesosiderites: Implications for exposure histories and production rates

A. ALBRECHT^{1†}, C. SCHNABEL^{1‡}, S. VOGT^{1§}, S. XUE^{1#}, G. F. HERZOG^{1*}, F. BEGEMANN², H. W. WEBER², R. MIDDLETON³, D. FINK^{3§} AND J. KLEIN³

¹Department of Chemistry, Rutgers University, New Brunswick, New Jersey 08903, USA

²Max-Planck-Institut für Chemie, D-55128 Mainz, Germany

³Department of Physics, University of Pennsylvania, Philadelphia, Pennsylvania 19104, USA

[†]Present address: Institute of Plant Sciences, ETH, Versuchsstation Eschikon, Eschikon 33, Postfach 185, CH-8315 Lindau, Switzerland

[‡]Present address: ETH Hoenggerberg, Institute of Particle Physics, HPK H21, CH-8093 Zurich, Switzerland

[§]Present address: IAEA, P.O. Box 200, Wagramerstrasse 5, A-1400 Vienna, Austria

[#]Present address: Graduate School of Oceanography, Narragansett Bay Campus, University of Rhode Island, Narragansett, Rhode Island 02882-1197, USA

^{*}Present address: ANSTO, PMB 1, Menai, NSW 2234, Australia

^{*}Correspondence author's e-mail address: herzog@rutchem.rutgers.edu

(Received 2000 January 3; accepted in revised form 2000 May 15)

Abstract—We report measurements of ²⁶Al, ¹⁰Be, ⁴¹Ca, and ³⁶Cl in the silicate and metal phases of 11 mesosiderites, including several specimens each of Budulan and Estherville, of the brecciated meteorite Bencubbin, and of the iron meteorite Udei Station. Average production rate ratios (atom/atom) for metal phase samples from Estherville and Budulan are ²⁶Al/¹⁰Be = 0.77 ± 0.02; ³⁶Cl/¹⁰Be = 5.3 ± 0.2. For a larger set of meteorites that includes iron meteorites and other mesosiderites, we find ²⁶Al/¹⁰Be = 0.72 ± 0.01 and ³⁶Cl/¹⁰Be = 4.5 ± 0.2. The average ⁴¹Ca/³⁶Cl production rate ratio is 1.10 ± 0.04 for metal separates from Estherville and four small iron falls. The ⁴¹Ca activities in dpm/(kg Ca) of various silicate separates from Budulan and Estherville span nearly a factor of 4, from <400 to >1600, indicating preatmospheric radii of >30 cm. After allowance for composition, the activities of ²⁶Al and ¹⁰Be (dpm/kg silicate) are similar to values measured in most ordinary chondrites and appear to depend only weakly on bulk Fe content. Unless shielding effects are larger than suggested by the ³⁶Cl and ⁴¹Ca activities of the metal phases, matrix effects are unimportant for ¹⁰Be and minor for ²⁶Al.

Noble gas concentrations and isotopic abundances are reported for samples of Barea, Emery, Mincy, Morristown, and Marjalahti. New estimates of ³⁶Cl/³⁶Ar exposure ages for the metal phases agree well with published values. Neon-21 production rates for mesosiderite silicates calculated from these ages and from measured ²¹Ne contents are consistently higher than predicted for L chondrites despite the fact that the mesosiderite silicates have lower Mg contents than L chondrites. We suggest that the elevation of the ²¹Ne production rate in mesosiderite silicates reflects a "matrix effect," that is, the influence of the higher Fe content of mesosiderites, which acts to enhance the flux of low-energy secondary particles and hence the ²¹Ne production from Mg. As ¹⁰Be production is relatively insensitive to this matrix effect, ¹⁰Be/²¹Ne ages give erroneously low production rates and high exposure ages. By coincidence, standard ²²Ne/²¹Ne based "shielding" corrections give fairly reliable ²¹Ne production rates in the mesosiderite silicates.

INTRODUCTION

When cosmic rays bombard extraterrestrial materials, they produce cosmogenic nuclides such as stable ²¹Ne and radioactive ¹⁰Be. The production rates, P , of these nuclides help in interpreting the irradiation histories of lunar rocks and meteorites. The production rates depend on both the geometric conditions under which the irradiation occurs (shielding) and the elemental composition of the target material. Equation (1) shows the conventional, empirical way to represent the shielding and composition dependencies of the production rate,

$$P = f \sum_i A_i N_i \quad (1)$$

Here the factor f takes account of shielding, N_i denotes the elemental abundance of each target element i , and the coefficient A_i can be loosely regarded as elemental production rates. Equation (1) is simple and has found wide use in the treatment of nuclides produced primarily by high- and intermediate-energy spallation reactions: ²⁶Al, ¹⁰Be, ⁵³Mn, and ²¹Ne. The equation incorrectly implies that production rates due to two different elements always stand in the

same ratio, A_i/A_j , to each other. Equation (2) gives the exact equation for the production rate:

$$P = \sum_i N_i \sum_j \int_0^{\infty} \sigma_{i,j}(E_j) \Phi_j(E_j) dE_j \quad (2)$$

The index j of the second summation runs over the various types of nuclear-active particles, mainly protons and neutrons. The term $\sigma_{i,j}(E_j)$ denotes the cross section for the nuclear reaction of particle j with nucleus i at energy E_j that gives rise to the product of interest; the term $\Phi_j(E_j)$ represents the flux of particles of type j with energy E_j . Examination of Eq. (2) shows that when more than one target element contributes significantly to total production of a nuclide, the effects of shielding and chemical composition cannot be so neatly separated as indicated by Eq. (1). As the geometric conditions of exposure change, so do the energy-dependent fluxes of the various nuclear-active particles, $\Phi_j(E_j)$, and in ways that depend on the composition of the target. Thus, if the cross sections of two target elements differ significantly in their dependence on bombarding particle energy, then the relative production rates of a nuclide made

from those two elements will vary from location to location as the energy spectrum of nuclear-active particles changes shape. In stony matter, the stable nuclide ^{21}Ne , for example, is produced mainly from the target elements Mg and Si. Particles with low energies play a larger role for ^{21}Ne production in the interactions with Mg than with Si. For this reason, the ratio $P_{\text{Mg}}(^{21}\text{Ne})/P_{\text{Si}}(^{21}\text{Ne})$ increases as the nuclear-active particles lose energy. The application of a shielding factor f cannot compensate for this kind of relative variation and, consequently, Eq. (1) does not always give the correct results. The relative variations of the coefficients A_i with bulk composition exemplify what is called the matrix effect.

How big is the matrix effect? The experimental evidence bearing on this question is limited. Begemann and Schultz (1988) have suggested that the relative production rates of ^{38}Ar from Ca and Fe vary by a factor of >3 . They have also considered the $^{22}\text{Ne}/^{21}\text{Ne}$ ratio, a key parameter measured with a precision of $<1\%$ and widely used to calculate the shielding factors, f , mentioned above. In meteorites with constant relative proportions of Mg, Al, and Si—the major target elements for Ne—but different bulk Fe contents, the $^{22}\text{Ne}/^{21}\text{Ne}$ ratios were seen to vary by 10%.

Theorists have also addressed the problem of the matrix effect. Masarik and Reedy (1994) have calculated for various compositions the ^{38}Ar production rate from Fe and Ca and the $^{22}\text{Ne}/^{21}\text{Ne}$ production rate ratio. In both cases, the results of their calculations confirm the size of the matrix effects inferred by Begemann and Schultz (1988). Michel *et al.* (1991) have examined the ^{26}Al and ^{21}Ne production rates in L and H chondrites, which contain about 22% and 27% of Fe, respectively. The calculated production rates of both ^{26}Al and ^{21}Ne are $\sim 7\%$ larger in L than in H chondrites. According to Michel and coworkers, an equation in the form of Eq. (1) adequately explains these variations: in effect, Fe acts simply as a diluent. Over this limited range of compositions, the matrix effect does not seem to play an important role.

Begemann and Schultz (1988) reached their conclusions about the matrix effect on ^{38}Ar production rates in a study of mesosiderites (Begemann *et al.*, 1976). The mesosiderites are brecciated, stony-iron meteorites consisting of variable amounts of metal and silicate. The silicates comprise mainly olivine, pyroxene, and calcic plagioclase (Dodd, 1981). The mesosiderites are a good place to look for a matrix effect because of the large variation in the fraction of Fe they contain. Mason and Jarosewich (1973) claim that the metal content ranges from 17% to 80%, although values between 40% and 60% are more typical. That variations in total Fe content are potentially important is indicated by calculations such as those of Michel *et al.* (1991) and Masarik and Reedy (1994), which confirm that cosmic-ray interactions with Fe produce a larger number of low-energy secondary particles than do interactions with lighter elements. Thus, targets richer in Fe give rise to "softer" particle fluxes that favor lower energies.

To obtain more information about the matrix effect, we have extended the mesosiderite study of Begemann *et al.* (1976). Here we present new measurements of the light noble gases and the nuclides: ^{26}Al (half life ($T_{1/2}$) = 0.705 Ma), ^{10}Be ($T_{1/2}$ = 1.5 Ma), ^{36}Cl ($T_{1/2}$ = 0.3 Ma), ^{41}Ca ($T_{1/2}$ = 0.1 Ma). The main purposes of the study were to evaluate the matrix effect for ^{26}Al and ^{10}Be and to reassess the exposure ages of mesosiderites in light of the results.

EXPERIMENTAL METHODS

Samples

The samples selected and their sources are identified in Table 1. Much but not all of the material came from specimens previously

studied by Begemann *et al.* (1976), who had separated metal and silicate phases magnetically from bulk samples. We will refer to these samples as the original group. We added to the original group four specimens of Budulan (2356, 2357, 2428, and 2459) and five specimens of Estherville received through the courtesy of M. Petaev and R. Clarke, Jr., respectively. Although Bencubbin is not a mesosiderite (Weisberg *et al.*, 1990), its metal-rich composition makes it suitable for inclusion in this study.

Mineral Separations

Portions of all samples in the original group were analyzed for ^{10}Be and ^{26}Al without additional purification. In cases for which sufficient material was available, we purified the metal-rich samples for ^{36}Cl analyses by repeated etching with 49% HF. The new samples of Budulan and Estherville were crushed and then separated into metal- and silicate-rich portions with a hand magnet. The metal-rich samples were purified by etching with HF.

Noble Gas Measurements

Table 2 shows the results of the new noble gas analyses together with published data for the same meteorites (Begemann *et al.*, 1976). For all seven meteorites, the concentrations of cosmogenic components as well as their abundance ratios are within the ranges reported previously. The same observation holds for the chemical compositions (Table 3) of the new samples. The measured $^{21}\text{Ne}/^{38}\text{Ar}$ ratios of the metal fractions from Estherville and Budulan are close to values typical of iron meteorites, ~ 0.2 . The similarity indicates that these metal separates contained only small amounts of silicate contamination.

Measurements of Cosmogenic Radionuclides and Chemical Composition

The procedures used to separate the cosmogenic radionuclides follow Vogt *et al.* (1991). To weighed portions of the silicate separates, we added known masses of Be (~ 2 mg), Al (~ 2 mg), Ca (~ 20 mg; larger quantities of Ca are needed for handling the metal and preparing the hydride), or all three as carriers. To the metal separates, we also added Cl (~ 5 mg) as NaCl. The silicates were dissolved in a solution of HF, HClO_4 , and HCl; the metal separates were dissolved with 7% HNO_3 only. The total masses of Ca and Al in the processed silicate samples included not only the added carrier but contributions from feldspars and other minerals. To determine the sizes of these contributions and for calculations of production rates, we took 10 mg aliquots of the samples for elemental analysis by direct-current atomic emission spectrometry (Feigenson and Carr, 1985).

With one set of exceptions, the ^{26}Al , ^{10}Be , ^{41}Ca , and ^{36}Cl in the samples were measured by accelerator mass spectrometry at the University of Pennsylvania. The methods used for ^{10}Be , ^{26}Al , and ^{41}Ca are described by Middleton and Klein (1986, 1987), and Fink *et al.* (1990), respectively; Vogt *et al.* (1993) outline the techniques employed for ^{36}Cl . The exceptions were certain metal-rich samples for which we analyzed the ^{36}Cl at PRIME Laboratory of Purdue University (see Table 1).

RESULTS AND DISCUSSION

Cosmogenic Radionuclides—Relation Between Activities and Production Rates

The measured activities of ^{26}Al , ^{10}Be , ^{36}Cl , and ^{41}Ca are given in Table 1. These activities equal production rates in space if (1) the

TABLE 1. Aluminum-26, ¹⁰Be, ⁴¹Ca, and ³⁶Cl (dpm/kg)* in mesosiderites, Bencubbin, and Udei Station.

Meteorite	Source ⁽¹⁾	ID ⁽²⁾	Silicate				Metal			
			²⁶ Al	¹⁰ Be	⁴¹ Ca	³⁶ Cl	²⁶ Al	¹⁰ Be	⁴¹ Ca	³⁶ Cl ⁽³⁾
Barea†	MNCN	St V	102	24.8	—	11.0 ⁽⁴⁾	7.7	5.7 ⁽⁵⁾	—	23.0 ± 0.6 ⁽⁶⁾ 24.9 ± 1.0 ⁽⁴⁾
Bencubbin	W 12155c	St ⁽⁷⁾	67.9	26.3	—	—	—	5.0	—	—
	W 12155c	—	—	—	—	—	7.4	4.9 ⁽⁸⁾	—	24.3 ± 1.5 ⁽⁴⁾
Bondoc	A(2)684.9	—	—	—	—	—	0.78	1.0	—	3.71 ± 0.17 3.2 ± 0.7 ⁽⁴⁾
Bondoc II	A(2)684.87	—	—	—	—	—	0.31	0.47	—	1.52 ± 0.07 1.5 ± 0.3 ⁽⁴⁾
Budulan	Mo2356	St	67.9	18.4	14.9	—	3.1	4.0	12.7	18.1 ± 0.5 ⁽⁶⁾
Budulan	Mo2357	St	71.3 ⁽⁹⁾	18.9	25.0	—	2.25	3.2 ⁽¹¹⁾	13.7	14.6 ± 1.5 ⁽¹⁰⁾ 16.6 ± 0.5 ⁽⁶⁾
Budulan	Mo2428	St	84.4	19.6	15.3	—	3.0	3.6	—	17.4 ± 1.7 ⁽¹⁰⁾ 18.8 ± 0.5 ⁽⁶⁾
Budulan	Mo2432+2439	St II	98.9	18.2	—	—	—	2.4	—	15.6 ± 0.4 ⁽⁶⁾ 13.7 ± 3.0 ⁽⁴⁾
Budulan	Mo2432+2439	St II ⁽⁷⁾	85.1	20.3	—	18.5 ⁽⁴⁾	2.8	3.3	—	—
Budulan	Mo2459	St	72.3	16.5	31.0	—	2.5	3.2	17.2 ⁽¹²⁾	17.5 ± 1.8 ⁽¹⁰⁾ 17.0 ± 0.6 ⁽⁶⁾
Clover Spr.	A646.4	—	—	—	—	13.4 ⁽⁴⁾	8.1	5.2	—	23.0 ± 0.9 ⁽⁶⁾ 23.9 ± 1.3 ⁽⁴⁾
Crab Orch.	Me1262	—	—	—	—	—	7.9	5.0	—	15.7 ± 0.7 ⁽⁶⁾ 17.3 ± 1.5 ⁽⁴⁾
Crab Orch.	Me1262	St ⁽⁷⁾	76.0	23.8	—	—	3.0	4.2	—	—
Emery	A H82.13	St II	48.5	27.0	—	13.7 ⁽⁴⁾	7.4	6.9	—	21.2 ± 0.8 ⁽⁶⁾
Emery	A H82.13	St V	66.9	23.4	—	—	—	—	—	22.2 ± 0.8 ⁽⁶⁾
Emery	A H82.13	St ⁽⁷⁾	78.0	21.6	—	—	4.2	6.0	—	24.0 ± 1.0 ⁽⁴⁾
Estherville†	N664	St	87.5	25.0	17.4 ⁽¹⁵⁾	—	—	2.6	19.8 ⁽¹⁵⁾	16.8 ± 1.7 ⁽¹⁰⁾ 17.9 ± 0.7 ⁽⁶⁾
Estherville	N1025A	St ⁽¹³⁾	84.9	20.6	14.0	—	2.8	3.8	23.1	18.8 ± 1.9 ⁽¹⁰⁾ 19.7 ± 0.8 ⁽⁶⁾
Estherville	N1025B	St	83.8	19.0	44.5	—	2.3	3.3	17.4	14.7 ± 1.5 ⁽¹⁰⁾
Estherville	N1025C ⁽¹⁴⁾	St I	73.6	17.5	18.4	—	2.9	3.5	21.5	16.5 ± 1.6 ⁽¹⁰⁾
Estherville	N1025C ⁽¹⁴⁾	St II	77.8	18.1	57.9	—	—	—	—	16.4 ± 0.5 ⁽⁶⁾
Estherville	N3311	St	83.4	19.3	21.0	—	2.2	3.2	—	16.2 ± 1.6 ⁽¹⁰⁾ 15.9 ± 0.7 ⁽⁶⁾
Mincy	NM F6248	St II	56.3	26.2	—	—	5.7	4.1	—	18.9 ± 1.5 ⁽⁴⁾
Mincy	NM F6248	St V	100.6	25.8	—	—	—	—	—	—
Mincy	NM F6248	St ⁽⁷⁾	59.5	22.5	—	—	3.0	5.3	—	—
Morristown	Me 1282	St V	80.0	19.7	—	12.5 ⁽⁴⁾	5.0	5.9	—	23.3 ± 1.1 ⁽⁶⁾ 20.2 ± 1.7 ⁽⁴⁾
Udei Station†	NASA	—	—	—	—	—	3.3	4.6	—	22.3 ± 1.1 ⁽⁶⁾ 19.6 ± 0.8 ⁽⁴⁾
Udei Station†	NASA	St ⁽⁷⁾	85.1	22.1	—	—	3.8	4.9	—	—
Vaca Muerta	Me 188	—	—	—	—	—	2.1	2.7	—	12.5 ± 0.6 ⁽⁶⁾ 13.3 ± 1.0 ⁽⁴⁾
Vaca Muerta	H300.16	St ⁽⁷⁾	45.2	10.9	—	—	1.6	2.4	—	—
Veramin†	Me 1269	—	—	—	—	—	4.2	4.9	—	23.6 ± 2.0 ⁽⁴⁾

*The 1σ uncertainties are 6–8% for ²⁶Al and ¹⁰Be and 10% for ⁴¹Ca.

†Observed fall.

(1) Sources of samples: A = American Meteorite Laboratory; MNCN = Museo Nacional de Ciencias Naturales, Madrid; Me = Field Museum of Natural History, Chicago (Dr. E. Olsen); Mo = Museum of Academy of Sciences, Moscow (Drs. Yu. A. Shukolyukov and M. Petaev); N = National Museum of Natural History, Washington, D.C. (Dr. R. Clarke, Jr.); NM = Naturhistorisches Museum, Vienna (Dr. G. Kurat); W = Western Australian Museum, Perth (D. Merrilees). (2) Mineral phases: St = silicate separate. The roman numerals designate different batches of silicate samples separated from one sample. We separated the silicates from Estherville and all Budulan samples, except Mo2432+2439. All other silicates were separated by Begemann *et al.* (1976). (3) Chlorine-36 activities were analyzed in samples different from the ones analyzed for ¹⁰Be and ²⁶Al. Additional determinations of ³⁶Cl in various samples of Bondoc, Dalgara, and Estherville are listed by Nishiizumi (1987). (4) Begemann *et al.* (1976). (5) Average of 5.71 and 5.76 dpm/kg. (6) Measured at PRIMELAB, Purdue University. (7) Nagai *et al.* (1993). All samples except Mincy supplied by F. Begemann. (8) Average of 4.5 and 5.3 dpm/kg. (9) Average of 71.2 and 71.3 dpm/kg. (10) Measured at the University of Pennsylvania. (11) 3.0 and 3.4 dpm/kg. (12) Average of 15.0 and 19.3 dpm/kg. (13) Beryllium-10 = average of 20.2 and 21.1; ²⁶Al = average of 81.6 and 88.2. (14) Results for ²⁶Al and ¹⁰Be were published previously under sample name 1026,6g by Albrecht *et al.* (1992); ⁴¹Ca results were given by Fink *et al.* (1991) under the name 1025. (15) Fink *et al.* (1991).

TABLE 2. Noble gas concentrations (10^{-8} cm³ STP/g) in silicate-rich and metal-rich phases separated from Barea, Budulan, Emery, Estherville, Mincy, Morristown, and Marjalahti.

Meteorite	³ He	⁴ He	$\frac{^{20}\text{Ne}}{^{21}\text{Ne}}$	²¹ Ne	$\frac{^{22}\text{Ne}}{^{21}\text{Ne}}$	$\frac{^{36}\text{Ar}}{^{38}\text{Ar}}$	³⁸ Ar	⁴⁰ Ar	⁸⁴ Kr	¹³² Xe
Barea St V*	17.5	1261	0.933	4.34	1.071	1.121	1.58	636	0.054	0.024
Barea St	16.5	1210	0.928	4.42	1.059	1.127	1.57	663	—	—
Budulan 2356, metal*	23.6	196	0.916	0.403	1.067	0.673	1.71	42	0.0042	0.0012
Budulan 2356, silicate*	45.2	1793	0.887	12.38	1.035	0.722	2.41	397	0.017	0.0036
Budulan 2459, metal*	28.2	150	0.930	0.373	1.062	0.649	2.02	36	0.0040	0.0010
Budulan 2459, silicate*	52.9	962	0.875	15.10	1.021	0.700	2.28	306	0.013	0.0024
Budulan 2459, silicate*	39.3	1396	0.888	10.99	1.029	0.832	3.08	652	0.046	0.013
Budulan, metal	28.3	190	1.478	0.387	1.109	0.738	1.87	102	—	—
Budulan, St I	44.6	1340	0.902	13.30	1.023	0.737	2.81	461	—	—
Budulan, St II	53.4	1029	0.885	14.80	1.027	0.711	2.28	270	—	—
Emery St V*	180.5	3010	0.897	39.8	1.050	0.686	24.37	918	0.034	0.0050
Emery St I	156.0	1040	0.905	32.6	1.064	0.680	29.40	445	—	—
Emery St II	333.0	2030	0.825	95.9	0.994	0.706	2.21	44	—	—
Emery St III	132.0	1270	0.900	27.1	1.070	0.643	25.50	1090	—	—
Estherville 1025 B, metal*	65.8	340	0.929	0.862	1.051	0.637	4.18	37	0.0059	0.0010
Estherville 1025 B, silicate*	88.4	1967	0.891	19.51	1.046	0.694	7.70	1181	0.035	0.0087
Mincy St V*	64.1	1764	0.898	15.7	1.055	0.743	4.13	812	0.022	0.0058
Mincy St I	53.5	1630	1.057	14.0	1.079	0.864	4.04	800	—	—
Mincy St I	61.2	1700	0.915	15.3	1.046	0.749	3.87	766	—	—
Mincy St II	88.9	1028	0.954	28.1	1.021	0.945	1.65	284	—	—
Morristown St V*	46.6	669	0.928	9.34	1.105	0.789	3.83	577	0.032	0.0075
Morristown St	43.5	656	1.030	8.96	1.127	0.890	4.35	587	—	—
Morristown St	47.7	721	1.010	8.88	1.096	0.807	4.93	713	—	—
Marjalahti St II*	357.0	1869	0.866	101.2	1.007	0.893	1.64	158	0.018	0.0034
Marjalahti St	340.0	1760	0.865	97.6	1.015	0.839	1.61	136	—	—
Marjalahti St	368.0	1929	0.856	105.0	1.010	0.794	1.36	49	—	—

*This work. Other analyses from Begemann *et al.* (1976). Uncertainties: in concentrations, $\pm 5\%$; in isotope ratios, $\pm 1\%$.

parent meteoroids had long single-stage exposure ages (*i.e.*, underwent constant irradiation by cosmic rays for times long compared to the half-lives of the radionuclides); and (2) the meteorites had short terrestrial ages (*i.e.*, landed too recently for the radionuclides to have decayed appreciably). Begemann *et al.* (1976) present exposure ages for the meteorites of Table 1. Even the shortest exposure age, that of Barea (9 Ma), guarantees an irradiation long enough for ²⁶Al, ¹⁰Be, ⁴¹Ca, ³⁶Cl, and ⁵⁹Ni ($T_{1/2} = 0.076$ Ma) to equal production rates, assuming one-stage exposures. Begemann *et al.* (1976) also summarize the data relevant to terrestrial ages. They conclude that of the 13 meteorites listed in Table 1 only 4—Budulan, Crab Orchard, Mincy, and Vaca Muerta—might have terrestrial ages long enough to have affected the observed activities appreciably.

Assuming the absence of any matrix effect or shielding effect on the ratio of the production rates of ³⁶Cl and ⁴¹Ca in the metal phase (see below), Eq. (3) gives us one way to calculate a terrestrial age for Budulan.

$$t_{\text{terr}} = \frac{1}{(\lambda_{41} - \lambda_{36})} \ln\left(\frac{r_{\text{Falls}}}{r_{\text{Budulan}}}\right); r = \frac{^{41}\text{Ca}}{^{36}\text{Cl}} \quad (3)$$

Figure 1 shows the ⁴¹Ca and ³⁶Cl activities of Budulan, the fall Estherville (this work), and several small iron falls (Fink *et al.*, 1991). The inferred ⁴¹Ca/³⁶Cl activity ratios are 1.23 ± 0.03 for Estherville alone, 1.10 ± 0.04 for the pooled data for Estherville and the iron falls, and 0.85 ± 0.09 for Budulan. The errors given are statistical and are perhaps unrealistically small. With $r_{\text{Falls}} = 1.23$, t_{terr} is 84 ± 22 ka and with $r_{\text{Falls}} = 1.10$, t_{terr} is 59 ± 22 ka.

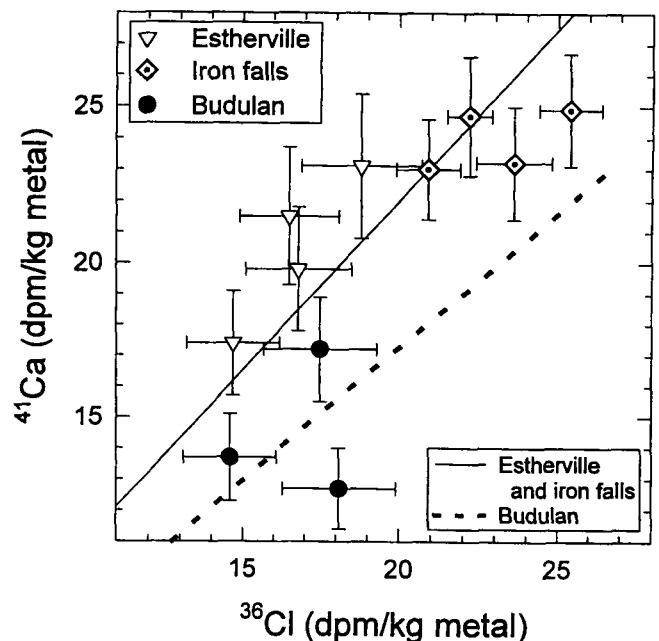


FIG. 1. The upper, solid line shows a best fit, forced through the origin, to data for the mesosiderite fall Estherville and for four small iron meteorites (Fink *et al.*, 1991). The lower line shows the best fit to data for samples of the Budulan find. The lower slope for Budulan indicates a terrestrial age of ~ 60 ka. However, the use of the nuclides ³⁶Cl and ¹⁰Be gives a lower terrestrial age; see text.

TABLE 3. Composition of silicates from mesosiderites, Bencubbin, and Udei Station (mass%) and production rates (dpm/kg) of ^{26}Al and ^{10}Be .

	[O]*	Mg	Al	[Si]†	Ca	Ti	Mn	Fe	P_{26}	P_{10}
Barea St V	44.1	9.15	3.59	25.6	4.01	0.16	0.35	13.2	92.8	23.0
Barea St‡	43.1	10.0	4.5	24.0	4.4	–	–	14.5	93.4	22.7
Bencubbin‡	44.2	21.1	2.1	22.9	2.2	–	–	7.2	82.3	24.3
Bencubbin#	44.9	21.2	1.8	23.3	1.56	–	–	6.8	81.8	24.6
Budulan										
Mo2356	44.5	10.8	2.75	26.5	2.67	0.13	0.37	12.2	91.5	23.3
Mo2357	44.0	11.1	2.27	26.0	2.33	0.12	0.39	13.9	87.8	23.1
Mo2428	43.1	9.5	4.21	23.7	4.38	0.17	0.36	14.6	90.9	22.6
Mo2432+Mo2439‡	45.1	11.8	3.0	22.3	2.6	–	–	15.2	81.7	23.6
Mo2459	44.2	11.4	1.92	26.4	1.99	0.14	0.42	13.5	87.2	23.3
Clover Springs ρ‡	44.1	13.0	1.5	23.8	1.9	–	–	14.2	78.7	23.2
Crab Orchard‡	44.5	8.0	5.0	23.0	4.8	–	–	14.4	92.4	22.9
Crab Orchard#	44.2	9.0	4.2	25.8	2.4	–	–	14.0	96.0	23.1
Emery St II	44.1	21.0	0.14	23.1	0.18	0.30	0.34	14.3	72.9	24.4
Emery St II‡	42.8	24.2	0.1	18.8	0.2	–	–	13.6	62.1	24.0
Emery St V	44.8	6.85	5.38	26.5	5.41	–	0.37	10.8	103.4	23.0
Emery St#	44.9	7.7	5.5	26.4	3.2	–	–	11.8	103.6	23.3
Estherville										
N664	43.8	8.98	3.66	25.4	4.01	0.16	0.31	13.6	92.6	22.8
N1025A	43.5	10.56	3.27	24.6	3.50	0.14	0.34	14.1	89.0	22.9
N1025B	42.6	7.32	3.81	24.3	3.85	0.16	0.31	17.6	89.7	22.2
N1025C St I	–	–	–	–	1.85	–	–	20.2	–	–
N1025C St II	41.7	6.40	3.44	23.5	3.66	0.11	0.27	20.9	85.4	21.7
N3311	44.4	12.1	2.47	26.0	2.75	0.10	0.34	11.8	89.2	23.4
Mincy St II‡	42.2	25.2	1.9	19.8	1.4	–	–	9.2	74.3	24.0
Mincy St V	44.5	10.0	3.23	26.5	3.52	–	0.36	11.9	93.7	23.2
Mincy St#	44.8	11.2	2.45	27.0	2.44	–	–	11.6	91.4	23.5
Morristown St V	43.0	7.65	4.17	27.0	4.19	–	0.34	13.6	99.0	22.5
Udei Station‡	31.4	11.3	1.3	15.2	1.0	–	–	26.2	71.7	17.6
Vaca Muerta St‡	44.2	12.7	1.9	23.0	2.4	–	–	15.5	78.5	23.3
Vaca Muerta St#	40.2	6.2	2.46	22.3	1.76	–	–	26.6	76.9	21.1
L chondrite	37.7	15.2	1.10	18.7	1.28	0.07	0.22	21.8	63.7	20.9
H chondrite§	35.7	14.2	1.01	17.1	1.19	0.06	0.25	27.6	58.6	20.0
Howardites§	44.4	10.36	3.71	23.6	4.16	0.20	0.38	13.22	88.5	23.1

*Oxygen not measured; calculated by assuming oxides of the other elements sum to 100%.

†Silicon measured only in those samples analyzed by Begemann *et al.* (1976); in other cases, Si was calculated from the stoichiometric relation: $[\text{SiO}_2] = 100 - \{[\text{MgO}] + [\text{Al}_2\text{O}_3] + [\text{CaO}] + [\text{TiO}_2] + [\text{MnO}] + [\text{FeO}]\}$.

‡Analyzed by Begemann *et al.* (1976). Sample Mo2432+Mo2439 is an average of StI and StII. The Udei Station material also contained 13.6% S.

§Mason (1979).

#Nagai *et al.* (1993)

An alternative approach to the calculation of terrestrial ages is based on a direct analog of Eq. (3) but with ^{36}Cl and ^{10}Be activities in meteoritic metal (Chang and Wänke, 1969). By using an expression for $^{36}\text{Cl}/^{10}\text{Be}$ at the time of fall, (*i.e.*, for r_{Falls}) given by Lavielle *et al.* (1999) and applying least-squares methods to the ^{36}Cl and ^{10}Be data for our five samples of Budulan, we find a terrestrial age of 9 ± 25 ka. Below we will use the value 30 ± 30 ka for the terrestrial age of Budulan. Crab Orchard and Mincy have ^{36}Cl activities in the metal phase that are slightly lower than the canonical one of 22.1 ± 1.4 dpm/kg found in many meteorite falls (Nishiizumi, 1995). Whether the lowering owes to shielding effects, terrestrial age, or both is unclear. Use of the ^{10}Be - ^{36}Cl activities as indicated above gives a terrestrial age of 123 ka for Crab Orchard and of 63 ka for Mincy. Unfortunately, silicate contamination in the metal phases analyzed, as indicated by high $^{26}\text{Al}/^{10}\text{Be}$ ratios, may

well have raised the measured ^{10}Be activities, lowered the ^{36}Cl activities, and hence raised the calculated terrestrial ages. The $^{26}\text{Al}/^{10}\text{Be}$ ratios in metal from Bondoc, in contrast, do not appear to reflect such contamination. The $^{36}\text{Cl}/^{10}\text{Be}$ terrestrial ages of our two samples are 275 and 325 ka. Begemann *et al.* (1976) ruled out a long terrestrial age for Bondoc based on a measurement of ^{14}C . As K. Welten (pers. comm., 2000) has noted, the Bondoc sample analyzed for ^{14}C may have contained terrestrial weathering products rather than *bona fide* extraterrestrial ^{14}C . Further study of the terrestrial age of Bondoc would be useful. Reedy *et al.* (1993) concluded that Vaca Muerta has a terrestrial age less than a few thousand years based on measurements of ^{14}C in the silicate phase of that meteorite.

We conclude that with the possible exceptions of Crab Orchard, Mincy, and Bondoc, the measured activities of Table 1 should

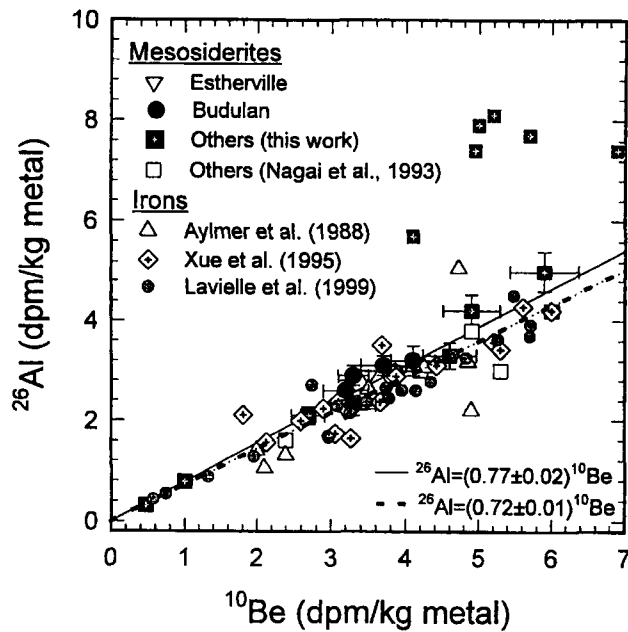
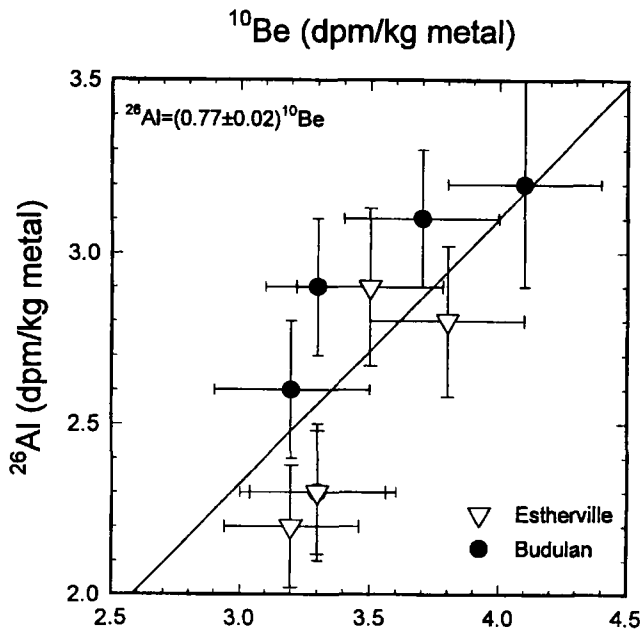


FIG. 2. The upper panel shows the ^{26}Al and ^{10}Be activities for the metal phases of Budulan and Estherville along with a best-fit line forced through the origin. Activities for Budulan have been corrected to the time of fall based on a terrestrial age of 30 ± 30 ka. For Budulan sample Mo2432+2439, we use the data of Nagai *et al.* (1993) because we did not determine ^{26}Al in the metal phase. The lower panel adds to the upper plot published data for iron meteorites, selected data for mesosiderites (see text), and a best-fit line (dotted) for all data, except the six squares (data points with crosshairs) that lie well above the plot because the metal separates contained some silicate. The $^{26}\text{Al}/^{10}\text{Be}$ ratios of the iron meteorites may be somewhat smaller either because the mesosiderite metal contains small amounts of contaminating silicates or because of terrestrial decay in some iron finds. The tenfold variation in activities can be understood in terms of shielding.

approximate production rates reasonably well. For Budulan, the one case in which we are confident that silicate contamination does not compromise the terrestrial age, measured activities are adjusted to the time of fall, namely, 30 ± 30 ka B.P. For simplicity, we begin

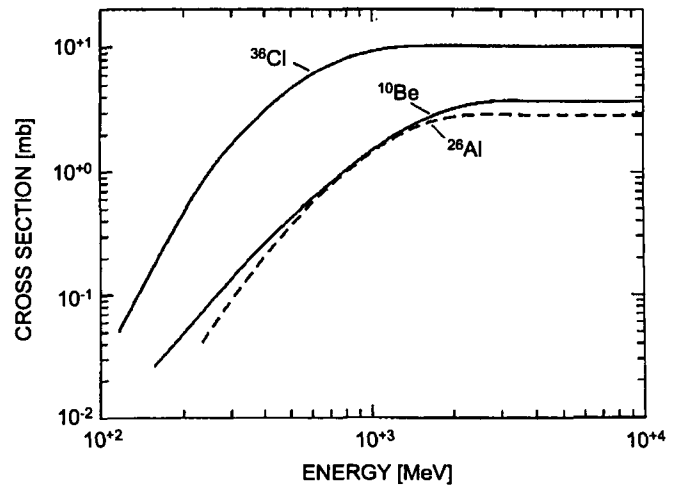


FIG. 3. The excitation functions for the reactions $\text{Fe}(p,x)^{10}\text{Be}$, $\text{Fe}(p,x)^{26}\text{Al}$, and $\text{Fe}(p,x)^{36}\text{Cl}$ (R. Michel, pers. comm.) show very much the same energy dependence. Hence, ratios of the production rates of ^{10}Be , ^{26}Al , and ^{36}Cl will exhibit no large variations within meteoroids of variable size and samples from various depths.

the detailed discussion of production rates with the metal-rich samples.

Production Rates of Cosmogenic Radionuclides in Metal-rich Material

Aluminum-26 and ^{10}Be —Figure 2 shows the ^{26}Al activities of the metal-rich samples plotted against the ^{10}Be activities. The upper panel (Fig 2a) includes only results for Estherville and Budulan and the best-fit line for the form $^{26}\text{Al} = k \times ^{10}\text{Be}$, which has the slope $k = (0.77 \pm 0.02)$. The lower panel (Fig. 2b) reprises the top one and adds to it data from four published sets of measurements. Nagai *et al.* (1993) have presented the ^{26}Al and ^{10}Be activities of metal separated from Crab Orchard, Emery, Mincy, Vaca Muerta, and the Udei Station iron meteorite; whereas Aylmer *et al.* (1988), Xue *et al.* (1995), and Lavielle *et al.* (1999) have measured the activities for numerous iron meteorites. Overall, the agreement with the trend inferred from the data for the mesosiderites Budulan and Estherville alone is remarkably good, in part because that best-fit line was forced through the origin.

Such agreement is not necessarily to be expected. For a sample at fixed depth, expressed in grams per centimeter squared in a meteoroid of fixed size, an increase in the total concentration of Fe and Ni should lead to an increase in the flux of low-energy secondary particles at the expense of the flux of higher-energy secondaries (*i.e.*, the energy spectrum of the nuclear-active particles should be softer in a metal-rich matrix relative to that in a metal-poor matrix). In the case of the production of ^{10}Be and ^{26}Al from Fe, however, the excitation functions for the proton-induced reactions are very much the same over the whole range of relevant proton energies (Fig. 3), and this similarity leaves room for neither a dependence on shielding conditions (Michlovich *et al.*, 1994) nor a matrix effect on the production rate ratio $P(^{26}\text{Al})/P(^{10}\text{Be})$. We infer that the higher ratios observed for some of the metal portions reported here (Barea, Bencubbin, Clover Springs, Crab Orchard, Emery, and Mincy) are artifacts caused by contamination of the metal with small quantities of silicates. In silicates, the $^{26}\text{Al}/^{10}\text{Be}$ ratio is $\sim 5\times$ higher than in metal which makes this ratio very sensitive to any such contamination. This explanation is supported by the observation that the metal

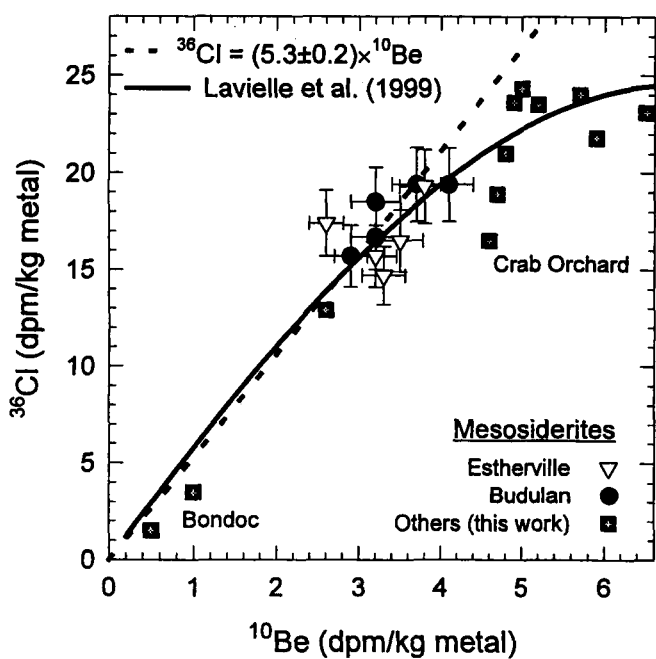


FIG. 4. Plot of ^{36}Cl vs. ^{10}Be in the metal phase from mesosiderites and in various irons. Data for Budulan have been corrected for a terrestrial age of 30 ± 30 ka. The dashed line is a best fit forced through the origin for Estherville and Budulan only. The solid curve has been proposed by Lavielle *et al.* (1999) and is based on analyses of iron meteorites.

fractions in question show evidence for an enhanced content of spallogenic ^{21}Ne , which is also much more abundantly produced in silicates than in metal. (This observation, unfortunately, rules out the possibility of calculating $^{10}\text{Be}/^{21}\text{Ne}$ ages for the metal phases, a possibility that may warrant further investigation in iron meteorites.) The presence of silicate in these samples is unsurprising inasmuch as they were analyzed without the much more rigorous etching procedures applied to the Budulan and Estherville separates.

A best-fit to all the data except for the metal samples contaminated by silicates (iron meteorites and mesosiderites) has the slope 0.72 ± 0.01 , a value that may be compared with the ratios of 0.68 ± 0.03 , 0.67 ± 0.10 , and 0.69 ± 0.02 obtained, respectively, from the results of Michlovich *et al.* (1994) for Canyon Diablo and of Xue *et al.* (1995) and Lavielle *et al.* (1999) for various iron meteorites. The ^{26}Al and ^{10}Be activities of the mesosiderites and the iron meteorites span comparable ranges, although the ^{26}Al and ^{10}Be activities of some samples from large iron meteorites are lower because of greater shielding. Nagai *et al.* (1999) report similar conclusions.

Chlorine-36 and ^{10}Be —Figure 4 shows the activities of ^{36}Cl and ^{10}Be in metal-rich samples. The dashed straight line is a regression, forced through the origin, for 10 pairs of measurements made for Budulan (corrected for terrestrial age) and Estherville. The slope, an estimate of the $^{36}\text{Cl}/^{10}\text{Be}$ production rate ratio for the shielding conditions relevant to these two meteorites, has the value 5.3 ± 0.2 . Vogt *et al.* (1990) cite $^{36}\text{Cl}/^{10}\text{Be}$ production rate ratios for metal of 4.6–5.7; Michlovich *et al.* (1994) obtained a ratio of 4.5 ± 0.2 for the Canyon Diablo iron meteorite.

Extrapolation of our dashed straight line to higher ^{10}Be activities leads to ^{36}Cl production rates above 25 dpm/kg. Such high ^{36}Cl production rates have not been observed in metal, implying that the $^{36}\text{Cl}/^{10}\text{Be}$ production rate ratio must decrease just as originally proposed by Nishiizumi *et al.* (1997) and later modified by Lavielle

TABLE 4. Metal contents of bulk meteorites.

Meteorite	Fe + Ni (%)
L chondrites*	23
H chondrites*	29
Mesosiderites†	
Barea	60
Budulan	73
Bondoc	47
Clover Springs	40
Crab Orchard	58
Emery	53
Estherville	59
Morristown	53
Vaca Muerta	50
Veramin	50
Average	54.3
Iron meteorites	100

*Mason (1979).

†Mason and Jarosewich (1973) plus 3% (see text).

et al. (1999). The solid curve in Fig. 4 depicts the correlation between the two production rates, which the latter authors deduced from data for iron meteorites. In general, the data for mesosiderites follow the trend line well, although in the case of Budulan the correction for terrestrial age introduces some circularity into this observation. As suggested above, Bondoc and Crab Orchard lie below the trend line in a region where it is hard to disentangle the effects of silicate contamination, terrestrial age, and experimental uncertainty.

In summary, two observations indicate that neither the ^{26}Al nor the ^{36}Cl production rate in the metal phase is subject to strong matrix effects: the near constancy in the metal phase of the $^{26}\text{Al}/^{10}\text{Be}$, and the consistency of the correlation of ^{36}Cl with ^{10}Be in mesosiderites and iron meteorites.

Production Rates of Aluminum-26 and Beryllium-10 in Silicates

We now examine the influence of matrix effects on the production rates of ^{10}Be and ^{26}Al in the silicate phases of mesosiderites. As noted above, any such influence should increase with increasing bulk Fe content of the mesosiderites. We will define matrix effects operationally as variations in production rates that cannot be understood in terms of compositional variations through the simple linear approximation of Eq. (1), shielding, or experimental uncertainty. To remove the effect of composition, we have divided the measured ^{10}Be and ^{26}Al activities (Table 1) by the relevant composition-dependent production rate. For ^{10}Be we use the production rate equation of Masarik and Reedy (1994),

$$P(^{10}\text{Be}) = 0.409 [\text{O}] + 0.17 [\text{Mg}] + 0.13 [\text{Al}] + 0.086 [\text{Si}] + 0.049 [\text{Fe}] \quad (4)$$

and for ^{26}Al that of Hampel *et al.* (1980),

$$P(^{26}\text{Al}) = 0.4 [\text{Mg}] + 4.92 [\text{Al}] + 2.74 [\text{Si}] + 0.24 [\text{Ca}] + 0.03 [\text{Fe}] \quad (5)$$

where production rates are in dpm/kg and elemental contents in mass %. In Fig. 5, we have plotted the $^{10}\text{Be}/P(^{10}\text{Be})$ and the $^{26}\text{Al}/P(^{26}\text{Al})$ ratios of mesosiderite silicates against the bulk Fe content (see Table 4) of the mesosiderite. In the absence of matrix effects and of systematic size effects, we would expect the data for

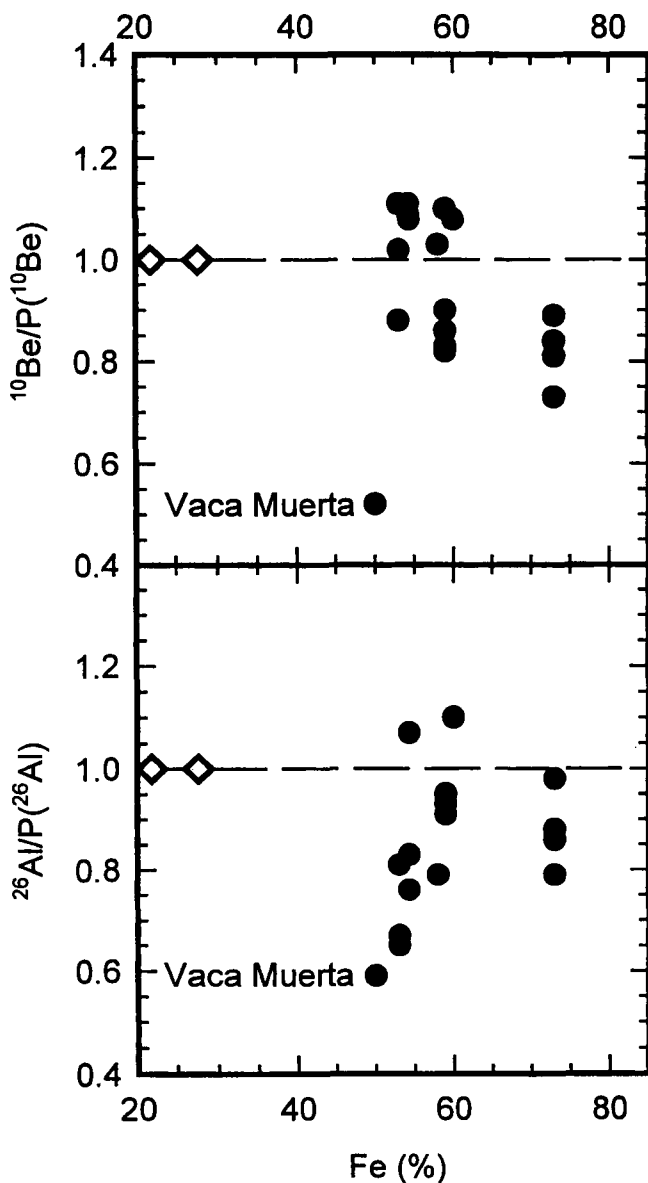


FIG. 5. The upper panel shows the ^{10}Be activities divided by the production rate expected on the basis of composition and normal shielding plotted against the bulk Fe content (Table 4). Filled circles are for the Fe-rich meteorites; open diamonds are for L and H chondrites. For Bencubbin and Mincy, we adopted the average Fe content of 54.3%. Uncertainties are estimated to be $\sim 10\%$. The points scatter near the value 1.0 with a grand average for mesosiderites of 0.94 ± 0.17 (the grand average includes the nine separately averaged values for specimens of Barea, Bencubbin, Budulan, Crab Orchard, Emery, Estherville, Mincy, Morristown, and Vaca Muerta). Vaca Muerta was evidently heavily shielded. No strong correlation is evident. The lower panel shows the corresponding plot for ^{26}Al . The variations due to shielding appear somewhat larger, but with most points falling in the range $0.8 \leq ^{26}\text{Al}/P(^{26}\text{Al}) \leq 1.0$. The grand average is 0.83 ± 0.15 . The ^{26}Al production rate does not appear to depend on the bulk Fe content.

each nuclide to scatter about a horizontal line parallel to the x axis at $y = 1$. This expectation is realized for the ^{10}Be data for which the average $^{10}\text{Be}/P(^{10}\text{Be})$ ratio is 0.94 ± 0.17 and no trend with Fe content is evident. The $^{26}\text{Al}/P(^{26}\text{Al})$ results are more ambiguous but at best furnish weak evidence for an increase with increasing Fe content. The average $^{26}\text{Al}/P(^{26}\text{Al})$ ratio is 0.87 ± 0.17 and r^2 for the best-fit line has a value of only 0.3. In considering the ^{26}Al results, it should be borne in mind that the points for ordinary

chondrites (Fe $\approx 25\%$) by definition plot at $^{26}\text{Al}/P(^{26}\text{Al}) = 1.0$, which is well above the trend line one might be tempted to extrapolate from the mesosiderite data. Thus, if all the results are to be understood in a single framework, and if the ^{26}Al data for the mesosiderites reflect any increase with Fe content because of the matrix effect, then that increase must be superimposed on a systematic depression of all mesosiderite ^{26}Al contents by heavy shielding. Apart from Vaca Muerta (and Bondoc, which is not included in this plot), the ^{10}Be data provide no evidence for a pervasive shielding effect. Further, after corrections for composition, a plot of $^{26}\text{Al}(\text{stone})/^{26}\text{Al}(\text{metal})$ vs. $^{10}\text{Be}(\text{stone})/^{10}\text{Be}(\text{metal})$ for the mesosiderites follows the trend predicted and observed by Welten *et al.* (1999) for 50 ordinary chondrites that are presumably in the normal shielding range ($3 < ^{10}\text{Be}(\text{stone})/^{10}\text{Be}(\text{metal}) < 5.4$). In summary, we believe that ^{26}Al production may rise slightly with increasing Fe content, but not by more than 25%. Such an effect does not compare in magnitude either with the one inferred by Begemann *et al.* (1976) for the ^{38}Ar production rate in the much more limited range of Fe contents defined by the mesosiderites alone or the one that affects ^{21}Ne production that we shall see below.

Calculation of Metal-phase Chlorine-36/Argon-36 Exposure Ages

For meteoritic metal, the most reliable cosmic-ray exposure age is that based on ^{36}Cl and ^{36}Ar . The method is so robust and straightforward that it has escaped the proliferation of improvements and refinements devised for most other cosmic-ray exposure dating systems. For meteorites with a single-stage exposure history and an exposure to cosmic rays lasting longer than ~ 1 Ma, only one parameter enters the calculations, namely, $P(^{36}\text{Cl})/[P(^{36}\text{Ar}) + P(^{36}\text{Cl})]$, which, together with the decay rate of ^{36}Cl , determines the total production of ^{36}Ar . In this expression, the term $P(^{36}\text{Ar})$ denotes only prompt or direct production of ^{36}Ar . According to Leya (1997), the ratio depends but little on the spectral shape of the nuclear-active particles: it varies only between 0.80 to 0.86 for all reasonable shielding conditions and all conceivable matrix effects. Taking into account the branching decay of ^{36}Cl —98.1% goes to ^{36}Ar —these values imply that the production ratio of total spallogenic ^{36}Ar to ^{36}Cl should be between 1.14 and 1.23. The relation between exposure age (Ma), spallogenic ^{36}Ar content (10^{-8} cm 3 STP/g) and ^{36}Cl activity, $A[^{36}\text{Cl}]$ (dpm/kg), is then given by

$$T_{36/36} = (430 \pm 16) \times [^{36}\text{Ar}]/A[^{36}\text{Cl}] \quad (6)$$

The numerical multiplication factor differs slightly but not significantly from the value of 425 that Begemann *et al.* (1976) used nor, indeed, from the one that Schaeffer and Heymann (1965) proposed in the first paper on this method. Lavielle *et al.* (1999) have independently estimated the value to be 427.

In Table 5, we have recalculated ^{36}Cl - ^{36}Ar exposure ages after averaging our new ^{36}Cl activities with published values and correcting the result for Budulan for a terrestrial age of 30 ka. The new and old results are virtually indistinguishable.

We emphasize that Eq. (6) holds only for meteoritic metal. In the silicate phases of mesosiderites and other meteorites, ^{36}Cl and ^{36}Ar will also be produced from Ca. Relative to Fe-Ni metal, nuclear reactions with Ca produce a larger fraction of ^{36}Ar directly and a smaller fraction indirectly from the decay of ^{36}Cl (Begemann *et al.*, 1976). Consequently, the multiplication factor in Eq. (6) becomes smaller for silicates. Specifically, assuming that the silicate phases have the same exposure ages as the respective metal,

TABLE 5. Cosmogenic ^{36}Ar and ^{36}Cl , and $^{36}\text{Cl}/^{36}\text{Ar}$ ages, $T_{36/36}$, of the metal phases of stony iron meteorites and Udei Station.

Meteorite	$^{36}\text{Ar}_c$ (10^{-8} cm 3 STP/g)	^{36}Cl (dpm/kg)	$T_{36/36}$ (Ma)
Barea	0.55 ± 0.04	24.0 ± 1.3	10 ± 1
Bondoc	1.25 ± 0.09	3.5 ± 0.4	156 ± 21
Bondoc II	0.56 ± 0.03	1.5 ± 0.1	159 ± 13
Average			158 ± 13
Budulan 2432+2439	1.15 ± 0.07	$15.7 \pm 1.3^*$	31 ± 3
Budulan 2356	1.07 ± 0.06	$19.4 \pm 0.5^*$	24 ± 2
Budulan 2459	1.27 ± 0.07	$18.5 \pm 0.9^*$	29 ± 3
Average			28 ± 1
Clover Springs	1.58 ± 0.10	23.5 ± 1.2	29 ± 3
Crab Orchard	2.62 ± 0.15	16.5 ± 1.1	68 ± 7
Emery	7.55 ± 0.40	22.9 ± 1.6	142 ± 11
Estherville†	3.30 ± 0.20	22.7 ± 2.2	63 ± 8
Estherville 1025B	2.63 ± 0.15	14.7 ± 1.5	77 ± 9
Average			70 ± 7
Lowicz	2.87 ± 0.10	23.0 ± 1.3	54 ± 4
Mincy	1.93 ± 0.13	18.9 ± 1.5	44 ± 5
Morristown	1.58 ± 0.10	21.8 ± 2.2	31 ± 4
Patwar	4.83 ± 0.25	23.0 ± 1.0	90 ± 7
Vaca Muerta	4.15 ± 0.20	12.9 ± 0.6	138 ± 11
Veramin	5.50 ± 0.25	23.6 ± 2.0	100 ± 10
Bencubbin	2.08 ± 0.20	24.3 ± 1.5	37 ± 4
Marjalahti	9.40 ± 0.40	22.2 ± 1.8	182 ± 18
Udei Station	6.00 ± 0.30	21.0 ± 1.9	123 ± 10

Notes: $^{36}\text{Ar}_c$ and ^{36}Cl from Begemann *et al.* (1976) and this work.*Corrected for decay assuming a terrestrial age of 30 ± 30 ka.

†Data from Schaeffer and Heymann (1965).

the data for the stony fractions of Barea, Emery, and Morristown yield values of ~ 120 . This value, in turn, implies that in these stone phases some 81% of the total ^{36}Ar is produced directly as compared to only 17% in the metal. As the exact percentage in any particular meteorite sample will depend on the Ca/Fe ratio and on the shielding conditions, the ^{36}Cl - ^{36}Ar method is rather unsuitable for stone meteorites and the stony portions of mesosiderites. A further complication arises from the possibility for producing some ^{36}Cl in stony meteorites through capture by ^{35}Cl of thermal and epithermal neutrons. Production by this route will increase the fraction of the total ^{36}Ar produced *via* the decay of ^{36}Cl and hence the multiplication factor in Eq. (6). Judged from the low values inferred for mesosiderite silicates, ~ 120 , as well as from the low measured $^{36}\text{Ar}/^{38}\text{Ar}$ ratios in all silicate samples, except Barea, ^{35}Cl (n,γ) ^{36}Cl reactions did not play a noticeable role in any of the meteorites investigated here.

Production Rates of Neon-21 in Silicates

In Table 6, we have divided the measured ^{21}Ne contents by the $^{36}\text{Cl}/^{36}\text{Ar}$ ages to obtain ^{21}Ne production rates for the samples. We now compare these actual values with ^{21}Ne production rates calculated in three ways (Table 6). In so doing, we assume that the metal and the silicate phases of each meteorite have had the same exposure history.

First, we have used the composition dependence of the production rate [10^{-8} cm 3 STP/(g-Ma)] as derived by Schultz and Freundel (1985) and adopted by Eugster and Michel (1995).

$$P^*(^{21}\text{Ne}) = 0.0163 [\text{Mg}] + 0.006 [\text{Al}] + 0.0032 [\text{Si}] + 0.0022 [\text{S}] + 0.0007 [\text{Ca}] + 0.00021 [\text{Fe} + \text{Ni}] \quad (7)$$

We have combined this expression with the "shielding correction"

$$P(^{21}\text{Ne}) = P^*(^{21}\text{Ne}) \times 6.4 \times [18.9 \times (^{22}\text{Ne}/^{21}\text{Ne}) - 14.9]^{-1} \quad (8)$$

suggested by Eugster and Michel (1995) for howardites. We chose howardites because, on average, their composition matches fairly well those of the silicates studied here (Table 3). It should be noted that the $^{22}\text{Ne}/^{21}\text{Ne}$ based "shielding factors" calculated from Eq. (8) depend implicitly on chemical composition. As different silicate portions from the same meteorite specimen may have quite different spallogenic $^{22}\text{Ne}/^{21}\text{Ne}$ ratios, the calculated shielding factors may differ appreciably, even though the physical shielding of the parent sample was the same throughout. For example, in the case of Emery, the shielding correction factors are 1.20 and 1.65 for Emery St III and St II, respectively.

The well-known tendency of shielding corrections based on the $^{22}\text{Ne}/^{21}\text{Ne}$ ratio alone to overestimate the ^{21}Ne production rates in chondrites with low $^{22}\text{Ne}/^{21}\text{Ne}$ ratios is observed in mesosiderites also: Bondoc is an extreme example. Otherwise, although the case-by-case agreement between the ^{21}Ne production rates from the formalism of Eugster and Michel (1995) on the one hand and from the ^{36}Cl - ^{36}Ar ages on the other is only fair, the overall agreement seems little short of remarkable (Fig. 6). To a large extent, this agreement results from correcting the nominal ^{21}Ne production rate

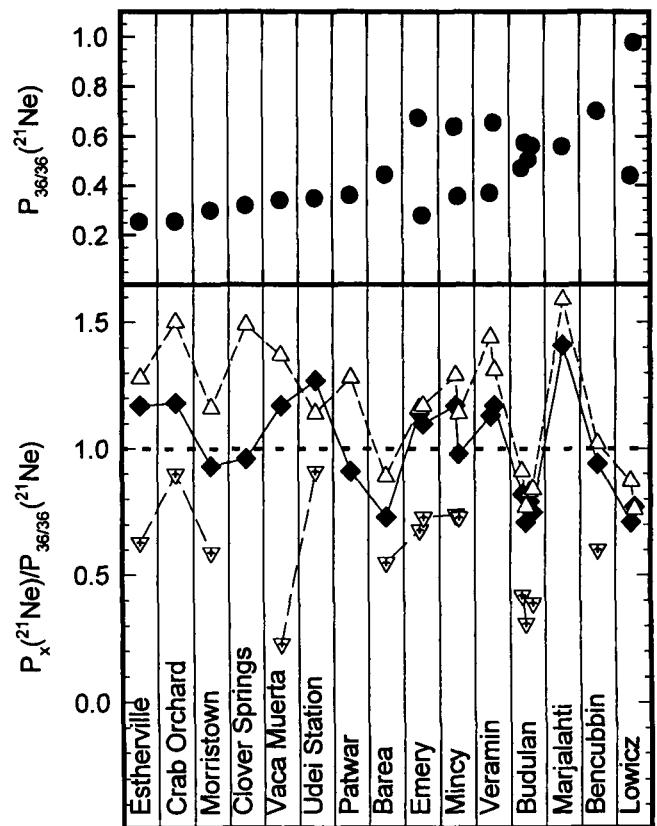


FIG. 6. Comparison of ^{21}Ne production rates calculated in different ways. The upper panel shows cosmogenic ^{21}Ne contents (10^{-8} cm 3 STP/g) measured in silicates divided by the $^{36}\text{Cl}/^{36}\text{Ar}$ cosmic-ray exposure ages (Ma) obtained for metal phases from the same meteorites, that is, a set of ^{21}Ne production rates, $P_{36/36}(^{21}\text{Ne})$. The appearance of more than one data point for a given meteorite indicates that several silicate samples with different chemical compositions were analyzed. The lower panel shows ratios to $P_{36/36}(^{21}\text{Ne})$ of ^{21}Ne production rates calculated in other ways, $P_x(^{21}\text{Ne})$. In particular, open triangles, solid diamonds, and inverted triangles with crosshairs, respectively, refer to calculations of $P(^{21}\text{Ne})$ based on the methods of Masarik and Reedy (1994), Eugster and Michel (1995), and Graf *et al.* (1990). Bondoc has been omitted because of exceptionally large shielding effects.

TABLE 6. Cosmogenic $^{21}\text{Ne}_c$ contents ($^{21}\text{Ne}_c$ in 10^{-8} cm 3 STP/g), $^{22}\text{Ne}/^{21}\text{Ne}$ ratios (atomic), and ^{21}Ne production rates (10^{-8} cm 3 STP/g-Ma).

	$^{21}\text{Ne}_c$	$^{22}\text{Ne}/^{21}\text{Ne}$	[1]	[2]	[3]	[4]
Barea	4.38	1.07	0.325	0.395	0.245	0.444
Bondoc	9.69	1.06	0.363	0.444	–	0.062
Bondoc II St I	10.50	1.01	0.624	0.674	–	0.066
Bondoc II St II	11.90	1.00	0.705	0.743	–	0.075
Budulan 2356	12.38	1.04	0.387	0.429	0.196	0.439
Budulan 2459	15.10	1.02	0.405	0.442	0.178	0.535
Budulan 2432+2439 St I	13.30	1.02	0.398	0.419	–	0.505
Budulan 2432+2439 St II	14.80	1.03	0.422	0.472	0.219	0.525
Clover Springs	9.30	1.12	0.308	0.478	–	0.321
Crab Orchard	17.40	1.08	0.301	0.382	0.229	0.255
Emery St II	95.9	0.99	0.770	0.781	0.460	0.675
Emery St V	39.8	1.05	0.309	0.328	0.204	0.280
Estherville 1025B	19.51	1.05	0.297	0.326	0.160	0.254
Lowicz St I	23.60	1.07	0.313	0.381	–	0.440
Lowicz St II	52.40	0.99	0.747	0.747	–	0.977
Mincy St II	28.10	1.02	0.746	0.824	0.476	0.640
Mincy St V	15.70	1.06	0.352	0.408	0.261	0.358
Morristown	9.34	1.10	0.277	0.347	0.177	0.299
Patwar	32.6	1.09	0.327	0.460	–	0.361
Vaca Muerta	47.20	1.04	0.400	0.468	0.079	0.341
Veramin St I	37.1	1.06	0.419	0.534	–	0.370
Veramin St II	65.6	1.01	0.764	0.856	–	0.655
Bencubbin	25.80	1.01	0.661	0.715	0.424	0.701
Marjalahti	102.0	1.01	0.792	0.892	–	0.560
Udei Station	43.00	1.00	0.443	0.397	0.319	0.350

References: [1] Calculated from composition and corrected for shielding through the $^{22}\text{Ne}/^{21}\text{Ne}$ ratio following Eugster and Michel (1995). [2] Calculated for depths of 10 to 12 cm in a mesosiderite with a radius of 20 cm assuming a density of 5.3 g/cm 3 (Masarik and Reedy, 1994). [3] Calculated from the ^{10}Be activity with corrections for composition but without other adjustments for shielding; see text. For Udei Station, we adjusted Eq. (10) to allow for the substantially lower O content because of the presence of S. [4] Calculated from the measured $^{21}\text{Ne}_c$ content (Begemann *et al.*, 1976, and Table 3) and the $^{36}\text{Cl}/^{36}\text{Ar}$ ages (Table 5).

for "shielding." In all cases, the spallogenic $^{22}\text{Ne}/^{21}\text{Ne}$ ratios are lower than the value of 1.127, which marks the divide between correction factors larger and smaller than 1.00, and, conventionally, between smaller and larger meteoroids, respectively. Thus, taken at face value, the low $^{22}\text{Ne}/^{21}\text{Ne}$ ratios would imply that during their exposure to cosmic radiation, all mesosiderites analyzed here were very much larger than "typical" chondritic meteoroids. Although some of the mesosiderites studied were undoubtedly large—Bondoc, Budulan, Estherville, Mincy, Vaca Muerta, and Udei Station—there is no evidence that all of them were. We suggest instead that the $^{22}\text{Ne}/^{21}\text{Ne}$ ratio does not distinguish changes in the spectra of cosmic-ray secondary particles that are due to shielding from those that are due to the matrix effect. By chance, it would appear, the matrix effect elevated the actual ^{21}Ne production rates to the level predicted by the Eugster and Michel formalism.

In a second computation of the ^{21}Ne production rates, we have followed the model calculations of Masarik and Reedy (1994), who attempt to take the matrix effect on ^{21}Ne production into account. For the silicates in mesosiderites, they arrive at elemental production rates for Al and Si that are nearly the same as in L chondrites. For Mg, however, they obtain a rate of ^{21}Ne production that is $\sim 1.8\times$ higher than in L chondrites. On average, the values of $P(^{21}\text{Ne})$ calculated from the results of Masarik and Reedy (1994) are 15% higher than those based on the $^{36}\text{Cl}/^{36}\text{Ar}$ ages and measured ^{21}Ne contents. It is interesting that these results are obtained without any individual adjustments for shielding effects: The calculated production rates hold for a depth of 53–62 g/cm 2 in a meteoroid with

a radius of 106.5 g/cm 2 . Thus, the overestimation of production rates suggests either that the importance of Mg as a target element is somewhat overestimated or that shielding is underestimated.

Finally, in our third set of calculations, we have followed Graf *et al.* (1990), who propose the relation shown below between the ^{10}Be and ^{21}Ne production rates (each in units of atoms mass $^{-1}$ time $^{-1}$) in L chondrites:

$$\frac{P(^{10}\text{Be})}{P(^{21}\text{Ne})} = 0.140 + 0.02 \times \left(\frac{^{22}\text{Ne}}{^{21}\text{Ne}} - 1.11 \right) \quad (9)$$

The dependence on irradiation hardness as measured by the $^{22}\text{Ne}/^{21}\text{Ne}$ ratio is quite weak. Even for the relatively extreme values $^{22}\text{Ne}/^{21}\text{Ne}$ of 1.30 and 1.05, the production rate ratio varies only from 0.144 to 0.139, respectively. In subsequent discussion, we shall adopt the L-chondrite value

$$\frac{P(^{10}\text{Be})}{P(^{21}\text{Ne})} = 0.141.$$

Before applying this relation to the mesosiderite silicates, some adjustments for composition are necessary. The production rate of ^{10}Be is higher in the mesosiderite silicates than in L chondrites because O, the most important target element for ^{10}Be production, is more abundant in the former, $\sim 44\%$ vs. 37.7% in L chondrites. Similarly, the production rate of ^{21}Ne in mesosiderite silicates varies appreciably with Mg and Si content. We allow for these compositional effects as shown in Eq. (10). Specifically, on setting $P(^{10}\text{Be})$

equal to the measured activity, $A[^{10}\text{Be}]$ and converting to measurement units (10^{-8} cm³ STP/g and dpm/kg), we find

$$P(^{21}\text{Ne}) = \frac{A[^{10}\text{Be}]}{0.141 \times 511} \times \frac{37.7}{44} \times \frac{P^*(^{21}\text{Ne})_M}{P^*(^{21}\text{Ne})_L} \quad (10)$$

$$= 0.0119 \times A[^{10}\text{Be}] \times \frac{P^*(^{21}\text{Ne})_M}{P^*(^{21}\text{Ne})_L}$$

where M and L denote mesosiderite silicates and L chondrites, respectively, and $P^*(^{21}\text{Ne})$ is defined in Eq. (7).

In all cases except Bondoc, which was excluded because of the unknown but large effect of shielding, the ^{21}Ne production rates derived from the ^{10}Be activities turn out to be too small. The deficiencies range between 10% (Crab Orchard) and a factor of 2 or more (Budulan). Clearly, the low ^{21}Ne production rates obtained from Eq. (10) do not result from low ^{10}Be activities: In the "olivines" in particular, the measured ^{10}Be activities are relatively high. We conclude that for the stony phase of mesosiderites the correlation between $P(^{21}\text{Ne})$ and $P(^{10}\text{Be})$ breaks down. Although the composition dependence of $P(^{10}\text{Be})$ is reasonably well described by any of several equations (see Moniot *et al.*, 1988), the production rate of ^{21}Ne is grossly underestimated. Such an underestimation is just what is expected from the enhanced number of low-energy, secondary, nuclear-active particles produced in the high-Z, Fe-rich matrix of mesosiderites.

An analogous treatment of the relationship between the production rates of ^{26}Al and ^{21}Ne defined by Graf *et al.* (1990), but with composition corrections to the ^{26}Al activities based on the production rate equation of Hampel *et al.* (1980), leads to $^{26}\text{Al}/^{21}\text{Ne}$ ages that are very close to the $^{10}\text{Be}/^{21}\text{Ne}$ ages. The similarities of the two sets of ages point to a much smaller matrix effect on ^{26}Al than on ^{21}Ne .

Constraints on the Preatmospheric Sizes of Estherville and Budulan—Leya *et al.* (2000) have used all available production cross sections to calculate production rates as a function of size and burial depth of several radionuclides, among them ^{36}Cl in meteoritic metal. Activities of ^{36}Cl in the range observed are predicted for mesosiderites with preatmospheric radii between about 35 cm and 50 cm (210 and 300 g/cm², assuming a density of 6 g/cm³). Similar radii, 35 ± 8 cm, are implied by the noble gas nuclide abundance systematics. To arrive at this value, we first calculated production rates of ^4He and ^{21}Ne from the contents of spallogenic ^4He (obtained after suitable corrections for radiogenic ^4He) and ^{21}Ne and the $^{36}\text{Cl}/^{36}\text{Ar}$ exposure ages, and then used the $P(^4\text{He})$ and $P(^{21}\text{Ne})$ vs. $^4\text{He}/^{21}\text{Ne}$ diagrams of Voshage (1984).

Calcium-41 from Calcium in Silicates from Budulan and Estherville

The main modes of production of ^{41}Ca in silicates are spallation of Fe and neutron capture by stable ^{40}Ca . The activity of ^{41}Ca due to the latter, ^{41}Ca in dpm/kg Ca, can be calculated from

$$^{41}\text{Ca} = (^{41}\text{Ca}_{\text{Silicate}} - ^{41}\text{Ca}_{\text{Metal}} \times [\text{Fe}_{\text{Silicate}}]) / [\text{Ca}_{\text{Silicate}}] \quad (11)$$

where square brackets denote mass fractions (Table 7). An uncertainty of unknown but potentially large size attaches to the value of $[\text{Ca}_{\text{Silicate}}]$, not because of instrumental problems, but because of the small size of the aliquots taken from this heterogeneous material for compositional analysis. In the one case we can test directly, Estherville N1025C St I and St II, the activities obtained are in poor

TABLE 7. Calcium-41 (dpm/[kg Ca]) in silicates from Budulan and Estherville.

Sample	^{41}Ca
Budulan*	
2428	368
2356	611
2357	1212
2459	1763
Estherville	
N1025A	307
N664	367
N3311	675
N1025B	1076
N1025C II	1465
N1025C I	760
Average 1025C	1115

*Corrected for a terrestrial age of 30 ka.

agreement, 760 vs. 1465 dpm/[kg Ca], and we assign an error of 30% to the average of 1115 dpm/[kg Ca].

We can use the maximum value of the ^{41}Ca activities for Budulan, ~1800 dpm/[kg Ca], and for Estherville, ~1500 dpm/[kg Ca], to estimate minimum preatmospheric radii for these meteorites. In the absence of theoretical production rates for ^{41}Ca , however, we first convert the ^{41}Ca activities to expected ^{59}Ni activities for which production rate calculations as a function of size and depth exist for L chondrites (Spergel *et al.*, 1986; Fig. 10). To a first approximation, the two activities should be related by the expression

$$^{41}\text{Ca} \text{ (dpm/[kg meteorite])} = ^{59}\text{Ni} \text{ (dpm/[kg meteorite])} \times \quad (12)$$

$$\sigma_{40} \times N_{40} / (\sigma_{58} \times N_{58})$$

where σ is the thermal neutron cross section and N is the number of atoms of the target nuclide (^{40}Ca or ^{58}Ni) per kilogram of meteorite. We choose ^{59}Ni for scaling over ^{36}Cl or ^{60}Co because the value of σ_{th}/I (the thermal neutron cross section divided by the resonance integral) for ^{59}Ni agrees best with the corresponding value for ^{41}Ca . Assuming a Ca content of 100% by mass in order to express ^{41}Ca activities in dpm/[kg Ca], we obtain the relation $^{41}\text{Ca} \text{ (dpm/[kg Ca])} = 15.4 \times ^{59}\text{Ni} \text{ (dpm/[kg meteorite with 1.2\% Ni])}$. With the maximum ^{41}Ca activities given above and an average density of 4.85 g/cm³ for mesosiderites (Buchwald, 1975), we find a minimum preatmospheric radius of 34 cm for Budulan and of 31 cm for Estherville. Although the measured ^{41}Ca activities are compatible with very large radii, we favor radii closer to the minimum inferred values because of the fairly normal ^{10}Be and ^{26}Al activities in the silicates. The assumed equivalence between radii of L chondrites and mesosiderites when depths are measured in grams per centimeter squared may or may not be valid. Although the total integrated neutron fluxes in L chondrites and iron meteorites appear to be similar (Spergel *et al.*, 1986; Fig. 7), relative to L chondrites the mesosiderites have lower fluxes of 100-eV neutrons (Spergel *et al.*, 1986; Fig. 6).

CONCLUSIONS

(1) The production rates of ^{26}Al and ^{10}Be in meteoritic metal appear to be much the same in mesosiderites, iron meteorites, and ordinary chondrites. The production rates do not depend on bulk composition of the bombarded object.

(2) After standard corrections for chemical composition, the production rates of ^{10}Be in the silicate phases of mesosiderites

appear to be much the same as in ordinary chondrites. Again no strong dependence on bulk composition is observed. Although the corresponding data for ^{26}Al have larger uncertainties, a matrix effect as large as the one observed for the production rate of ^{38}Ar from Ca is ruled out. A smaller increase is possible, perhaps 25% as bulk Fe content increases from that of ordinary chondrites to that of iron meteorites. Further study of silicate inclusions from iron meteorites could help define the size of this effect.

(3) On average, $^{10}\text{Be}/^{21}\text{Ne}$ exposure ages of the silicate phases are more than 60% higher than $^{36}\text{Cl}/^{36}\text{Ar}$ ages of the metal phases in mesosiderites. This observation suggests that the higher Fe contents of mesosiderites tend to raise ^{21}Ne production rates from Mg, which is consistent with suggestions by Begemann and Schultz (1988) and calculations by Masarik and Reedy (1994). Neon-21 exposure ages calculated for silicate inclusions from iron meteorites should therefore be interpreted with caution.

Acknowledgments—K. Chan assisted with sample preparation. R. Michel made available the cross section data depicted in Fig. 3, and Robert Reedy gave us useful advice. In refereeing this manuscript, Kees Welten, Don Bogard, and the associate editor made helpful comments. We thank them all. This work was supported in part by NASA Grant NAGW 34-99 IPAS.

Editorial handling: R. Wieler

REFERENCES

- ALBRECHT A., VOGT S., HERZOG G. F., MIDDLETON R., DEZFOULY-ARJOMANDY B., FINK D. AND KLEIN J. (1992) ^{26}Al , ^{10}Be , and ^{41}Ca in mesosiderites (abstract). *Lunar Planet. Sci.* **23**, 5–6.
- AYLMER D., BONANNO V., HERZOG G. F., WEBER H., KLEIN J. AND MIDDLETON R. (1988) ^{26}Al and ^{10}Be production in iron meteorites. *Earth Planet. Sci. Lett.* **88**, 107–118.
- BEGEMANN F. AND SCHULTZ L. (1988) The influence of bulk chemical composition on the production rate of cosmogenic nuclides in meteorites (abstract). *Lunar Planet. Sci.* **19**, 51–52.
- BEGEMANN F., WEBER H. W., VILCSEK E. AND HINTENBERGER H. (1976) Rare gases and ^{36}Cl in stony-iron meteorites: Cosmogenic elemental production rates, exposure ages, diffusion losses and thermal histories. *Geochim. Cosmochim. Acta* **40**, 353–368.
- BUCHWALD V. F. (1975) *Handbook of Iron Meteorites*. Univ. California Press, Berkeley, California, USA. 1418 pp.
- CHANG C. AND WÄNKE H. (1969) Beryllium-10 in iron meteorites: Their cosmic-ray exposure and terrestrial ages. In *Meteorite Research* (ed. P. M. Millman), pp. 397–401. D. Reidel, Dordrecht, The Netherlands.
- DODD R. T. (1981) *Meteorites, A Petrologic-Chemical Synthesis*. Cambridge Univ. Press, Cambridge, England. 368 pp.
- EUGSTER O. AND MICHEL T. (1995) Common asteroid break-up events of eucrites, diogenites, and howardites and cosmic-ray production rates for noble gases in achondrites. *Geochim. Cosmochim. Acta* **59**, 177–199.
- FEIGENSON M. D. AND CARR M. J. (1985) Determination of major, trace, and rare earth elements in rocks by DCP-AES. *Chem. Geol.* **51**, 19–27.
- FINK D., MIDDLETON R. AND KLEIN J. (1990) ^{41}Ca : Accelerator mass spectrometry and applications. *Nucl. Instrum. Methods* **B47**, 79–96.
- FINK D., KLEIN J., MIDDLETON R., VOGT S. AND HERZOG G. F. (1991) ^{41}Ca in iron falls, Grant, and Estherville: Production rates and related exposure age calculations. *Earth Planet. Sci. Lett.* **107**, 115–128.
- GRAF TH., BAUR H. AND SIGNER P. (1990) A model for the production of cosmogenic nuclides in chondrites. *Geochim. Cosmochim. Acta* **54**, 2521–2534.
- HAMPEL W., WÄNKE H., HOFMEISTER H., SPETTEL B. AND HERZOG G. F. (1980) ^{26}Al and rare gases in Allende, Bereba, and Juvinas: Implications for production rates. *Geochim. Cosmochim. Acta* **44**, 539–547.
- LAVIELLE B., MARTI K., JEANNOT J.-P., NISHIZUMI K. AND CAFFEE M. (1999) The ^{36}Cl - ^{36}Ar - ^{40}K - ^{41}K records and cosmic ray production rates in iron meteorites. *Earth Planet. Sci. Lett.* **170**, 93–104.
- LEYA I. (1997) Modellrechnungen zur Beschreibung der Wechselwirkungen galaktischer kosmischer Teilchenstrahlung mit Stein- und Eisenmeteoroiden.-Dünn-targetbestrahlungen und Dickt-targetexperimente. Ph.D. thesis, Universität Hannover, Germany. 459 pp.
- LEYA I., LANGE H.-J., NEUMANN S., WIELER R. AND MICHEL R. (2000) The production of cosmogenic nuclides in stony meteoroids by galactic cosmic ray particles. *Meteorit. Planet. Sci.* **35**, 259–286.
- MASARIK J. AND REEDY R. C. (1994) Effects of bulk composition on nuclide production processes in meteorites. *Geochim. Cosmochim. Acta* **58**, 5307–5317.
- MASON B. (1979) Chapter B. Cosmochemistry. Part 1. Meteorites. In *Data of Geochemistry, 6th Ed.* (eds. M. Fleischer, I. Friedman and J. R. O'Neil), pp. B1–B132. U.S. Geological Survey Prof. Paper **440-B-1**, U.S. Govt. Print. Office, Washington, D.C., USA.
- MASON B. AND JAROSEWICH E. (1973) The Barea, Dyarri Island, and Emery meteorites, and a review of the mesosiderites. *Mineral. Mag.* **39**, 204–215.
- MICHEL R., DRAGOVITSCH P., CLOTH P., DAGGE G. AND FILGES D. (1991) On the production of cosmogenic nuclides in meteoroids by galactic protons. *Meteoritics* **26**, 221–242.
- MICHOVICH E. S., VOGT S., MASARIK J., REEDY R. C., ELMORE D. AND LIPSCHUTZ M. E. (1994) ^{26}Al , ^{10}Be , and ^{36}Cl depth profiles in the Canyon Diablo iron meteorite. *J. Geophys. Res., Planets* **99**, 23 187–23 194.
- MIDDLETON R. AND KLEIN J. (1986) A new method for measuring $^{10}\text{Be}/^{9}\text{Be}$ ratios. In *Proc. Workshop Tech. Accel. Mass Spectrom.*, pp. 76–81. Oxford, England.
- MIDDLETON R. AND KLEIN J. (1987) ^{26}Al : Measurement and applications. *Phil. Trans. Royal Soc. London* **A323**, 121–143.
- MONIOT R. K., TUNIZ C., KRUSE T. H., SAVIN W., PAL D. K. AND HERZOG G. F. (1988) Production of ^{10}Be in stony meteorites: Composition dependence. *Geochim. Cosmochim. Acta* **52**, 499–504.
- NAGAI H., HONDA M., IMAMURA M. AND KOBAYASHI K. (1993) Cosmogenic ^{10}Be and ^{26}Al in metal, carbon and silicate of meteorites. *Geochim. Cosmochim. Acta* **57**, 3705–3723.
- NAGAI H., KOKUBO M., KOBAYASHI T. AND HONDA M. (1999) Cosmogenic ^{10}Be and ^{26}Al in iron meteorites and the inclusions (abstract). *Antarctic Meteorites* **24**, 116–118.
- NISHIZUMI K. (1987) ^{53}Mn , ^{26}Al , ^{10}Be and ^{36}Cl in meteorites: Data compilation. *Nucl. Tracks Radiat. Meas.* **13**, 209–273.
- NISHIZUMI K. (1995) Terrestrial ages of meteorites from hot and cold regions (abstract). In *Workshop on Meteorites from Cold and Hot Deserts* (eds. L. Schultz, J. O. Annexstad and M. E. Zolensky), pp. 53–55. LPI Tech. Report **95-02**, Lunar and Planetary Institute, Houston, Texas, USA.
- NISHIZUMI K., CAFFEE M. W., JEANNOT J.-P., LAVIELLE B. AND HONDA M. (1997) A systematic study of the cosmic-ray-exposure history of iron meteorites: Beryllium-10-Chlorine-36/Beryllium-10 terrestrial ages (abstract). *Meteorit. Planet. Sci.* **32** (Suppl.), A100.
- REEDY R. C., MASARIK J., JULL A. J. T., DONAHUE D. J. AND WASSON J. T. (1993) Studies of cosmic-ray-produced carbon-14 in the Vaca Muerta mesosiderite (abstract). *Meteoritics* **28**, 421–422.
- SCHAEFFER O. A. AND HEYMANN D. (1965) Comparison of ^{36}Cl - ^{36}Ar and ^{36}Ar - ^{38}Ar cosmic ray exposure ages of dated fall iron meteorites. *J. Geophys. Res.* **70**, 215–224.
- SCHULTZ L. AND FREUNDEL M. (1985) On the production rate of ^{21}Ne in ordinary chondrites. In *Isotopic Ratios in the Solar System*, pp. 27–33. Cepadues-Editions, Toulouse, France.
- SPERGER M. S., REEDY R. C., LAZARETH O. W., LEVY P. W. AND SLATEST A. (1986) Cosmogenic neutron-capture-produced nuclides in stony meteorites. *Proc. Lunar Planet. Sci. Conf. 16th, J. Geophys. Res. Suppl.* **91**, D484–D494.
- VOGT S., HERZOG G. F. AND REEDY R. C. (1990) Cosmogenic nuclides in extraterrestrial materials. *Rev. Geophys.* **28**, 253–275.
- VOGT S., HERZOG G. F., FINK D., KLEIN J., MIDDLETON R., DOCKHORN B., KORSCHINEK G. AND NOLTE E. (1991) Exposure histories of the lunar meteorites MacAlpine Hills 88104, MacAlpine Hills 88105, Yamato 791197 and Yamato 86032. *Geochim. Cosmochim. Acta* **55**, 3157–3165.
- VOGT S. ET AL. (1993) Exposure history of the lunar meteorite Elephant Moraine 87521. *Geochim. Cosmochim. Acta* **57**, 3793–3799.
- VOSHAGE H. (1984) Investigations of cosmic-ray-produced nuclides in iron meteorites. 6. The Signer-Nier model and the history of the cosmic radiation. *Earth Planet. Sci. Lett.* **71**, 181–194.
- WELTEN K. C., MASARIK J., NISHIZUMI K., CAFFEE M. W. AND WIELER R. (1999) The stone/metal ratios for ^{10}Be and ^{26}Al as empirical shielding parameters in ordinary chondrites (abstract). *Meteorit. Planet. Sci.* **34** (Suppl.), A121–A122.
- WEISBERG M. K., PRINZ M. AND NEHRU C. E. (1990) The Bencubbin chondrite breccia and its relationship to CR chondrites and the ALH 85085 chondrite. *Meteoritics* **25**, 269–279.
- XUE S., HERZOG G. F., SOUZIS A., ERVIN M. H., LAREAU R. T., MIDDLETON R. AND KLEIN J. (1995) Stable magnesium isotopes, ^{10}Be , ^{26}Al , and $^{26}\text{Mg}/^{26}\text{Al}$ exposure ages of iron meteorites. *Earth Planet. Sci. Lett.* **136**, 397–406.